

## BLAZARS SPECTRAL PROPERTIES AT 74 MHZ

F. MASSARO<sup>1</sup>, M. GIROLETTI<sup>2</sup>, A. PAGGI<sup>3</sup>, R. D'ABRUSCO<sup>3</sup>, G. TOSTI<sup>4,5</sup> & S. FUNK<sup>1</sup>.

version August 6, 2013: fm

### ABSTRACT

Blazars are the most extreme class of active galactic nuclei (AGNs). Despite a previous investigation at 102 MHz for a small sample of BL Lacs and our recent analysis of blazars detected in the Westerbork Northern Sky Survey (WENSS), a systematic study of the blazar spectral properties at frequencies below 100 MHz has been never carried out. In this paper, we present the first analysis of the radio spectral behavior of blazars based on the recent Very Large Array Low-Frequency Sky Survey (VLSS) at 74 MHz. We search for blazar counterparts in the VLSS catalog confirming that they are detected at 74 MHz. We then show that blazars present radio flat spectra (i.e., radio spectral indices  $\sim 0.5$ ) when evaluated also about an order of magnitude in frequency lower than previous analyses. Finally, we discuss the implications of our findings in the context of the blazars – radio galaxies connection since the low frequency radio data provide a new diagnostic tool to verify the expectations of the unification scenario for radio-loud active galaxies.

*Subject headings:* galaxies: active - galaxies: BL Lacertae objects - radiation mechanisms: non-thermal

### 1. INTRODUCTION

Blazars are compact, core-dominated, radio-loud sources characterized by highly variable, non-thermal, continuum that extends from radio to  $\gamma$ -rays. Their spectral energy distributions (SEDs) exhibit two main, broadly peaked, components: a low-energy one with its maximum between the IR and the X-ray band, and the high-energy one peaking in the  $\gamma$ -rays. Their emission also features high and variable polarization, apparent superluminal motions, and high apparent luminosities (e.g., Blandford & Rees 1978a; Urry & Padovani 1995). Recently, we discovered that their IR colors are clearly distinct from those of other extragalactic sources, in particular, when considering  $\gamma$ -ray blazars (see also Massaro et al. 2011a; D'Abrusco et al. 2012; D'Abrusco et al. 2013).

Blazars are generally divided in two main categories: the BL Lac objects, characterized by featureless optical spectra and low luminosity and the flat-spectrum radio quasars with optical spectra typical of quasars (see e.g., Stickel et al. 1991; Stoke et al. 1991; Laurent-Muehleisen et al. 1999, for more details on the optical classification). In the following we label the former class as BZBs and the latter as BZQs, adopting the nomenclature of the Multifrequency Blazar Catalog<sup>5</sup> (ROMA-BZCAT, Massaro et al. 2009), while blazars of uncertain type are indicated as BZUs.

Despite a survey of BZBs at 102 MHz (Artyukh & Vetukhnovskaya 1981), the low radio frequency spectral behavior of blazars is still an unexplored portion of the electromagnetic spectrum for

studying the blazar emission. We recently analyzed blazar data obtained with the Westerbork Synthesis Radio Telescope (WSRT), combining the archival observations present in the Westerbork Northern Sky Survey (WENSS; Rengelink et al. 1997) at 325 MHz with those of the NRAO Very Large Array Sky survey (NVSS; Condon et al. 1998) and of the Very Large Array Faint Images of the Radio Sky at Twenty-Centimeters (FIRST; Becker et al. 1995; White et al. 1997) at 1.4 GHz. We found that blazars have flat radio spectra also between 325 MHz and 1.4 GHz and on the basis of this result we proposed a new approach to search for  $\gamma$ -ray blazar candidates among the unidentified gamma-ray sources (UGSSs) detected by *Fermi* (see Massaro et al. 2013, for more details).

In this paper we extend our previous investigation of low radio frequency emission of blazars to frequencies below 100 MHz using the archival observations of the Very Large Array Low-Frequency Sky Survey<sup>6</sup> (VLSS; Cohen et al. 2007). The VLSS is a 74 MHz (4m) continuum survey covering the entire sky north of  $\sim 30^\circ$  declination. The entire survey region is covered with a resolution of  $\sim 80''$  with an average root mean square noise of 0.1 Jy/beam. We investigate the low-frequency spectral shape of blazars, with particular focus on those that are  $\gamma$ -ray emitters. A comparison between this VLSS analysis and that performed using the WENSS is also presented.

In the present work we aim at verifying if blazars maintain a flat radio spectrum even below 100 MHz. We will also test if their spectral properties are in agreement with the expectations of the unification scenario for radio-loud active galaxies which suggests that the observed differences between radio galaxies and blazars are mostly due to a different orientation along the line of sight (see Kharb et al. 2010, for a recent discussion on radio properties of blazars and radio galaxies in the context of the unification scenario).

The paper is organized as follows: in Section 2 we

<sup>1</sup> SLAC National Laboratory and Kavli Institute for Particle Astrophysics and Cosmology, 2575 Sand Hill Road, Menlo Park, CA 94025, USA

<sup>2</sup> INAF Istituto di Radioastronomia, via Gobetti 101, 40129, Bologna, Italy

<sup>3</sup> Harvard - Smithsonian Astrophysical Observatory, 60 Garden Street, Cambridge, MA 02138, USA

<sup>4</sup> Dipartimento di Fisica, Università degli Studi di Perugia, 06123 Perugia, Italy

<sup>5</sup> <http://www.asdc.asi.it/bzcat/>

<sup>6</sup> <http://lwa.nrl.navy.mil/VLSS/>

search for the counterparts of the blazars listed in the ROMA-BZCAT that lie in area covered by the VLSS while in Section 3 we describe the samples used in our analysis. Section 4 is devoted to description of the low-frequency radio spectral behavior for the VLSS blazars. Section 5 is dedicated to the discussion of our findings.

For our numerical results, we use cgs units unless stated otherwise and we assume a flat cosmology with  $H_0 = 72 \text{ km s}^{-1} \text{ Mpc}^{-1}$ ,  $\Omega_M = 0.26$  and  $\Omega_\Lambda = 0.74$  (Dunkley et al. 2009). Spectral indices,  $\alpha$ , are defined by flux density,  $S_\nu \propto \nu^{-\alpha}$ .

## 2. SPATIAL ASSOCIATIONS OF BLAZARS IN THE VLSS

The starting catalog used in our investigation is the ROMA-BZCAT v4.1, listing 3149 blazars (e.g. Massaro et al. 2011b)<sup>7</sup> distinct as 1220 BZBs (950 BL Lacs and 270 BL Lac candidates), 1707 BZQs and 222 blazars of uncertain type (BZUs). However, the ROMA-BZCAT blazars lying above declination  $\sim -30$  deg as in the VLSS survey are only 2727: 1115 BZBs, 1412 BZQs and 200 BZUs. In particular, 678 of them are  $\gamma$ -ray emitters: 349 BZBs, 282 BZQs and 47 BZUs as associated in the Second *Fermi* Large Area Telescope catalog and in the Second *Fermi* LAT Catalog of active galactic nuclei (2FGL, 2LAC; Nolan et al. 2012; Ackermann et al. 2011a, respectively).

The positional uncertainties on the coordinates reported in the ROMA-BZCAT are not uniform since they have been taken from different surveys but the accuracy on the blazar positions is of the order of  $1''$  with only several exceptions. Thus to identify low radio frequency counterparts of blazars at 74 MHz, we used the following approach, already successfully adopted to search for blazar counterparts in the WENSS (Massaro et al. 2013). We searched for all the ROMA-BZCAT correspondences in the VLSS within circular regions of different radii  $R$  ranging between  $0''$  and  $30''$ . To perform our investigation the VLSS catalog available on the HEASARC website<sup>8</sup> was used.

We calculated the number of correspondences  $N(R)$  as a function of  $R$ , and the difference between the number of associations at given radius  $R$  and those at  $(R - \Delta R)$ :

$$\Delta N(R) = N(R) - N(R - \Delta R), \quad (1)$$

where  $\Delta R = 0.5''$ . Figure 1 shows the curves corresponding to  $N(R)$  and  $\Delta N(R)$  as a function of  $R$ . We found that the number of VLSS sources positionally associated with ROMA-BZCAT blazars does not increase significantly (i.e.,  $\Delta N(R)$  systematically lower than 5), at radii larger than  $21''$ . This is also highlighted by the correspondent differential curve  $\Delta N(R)$ , clearly flat for radii greater than  $21''$  (see lower panel of Figure 1). Thus we chose the angular separation of  $21''$  as the radial association threshold  $R_A$  for assigning VLSS counterparts to ROMA-BZCAT blazars.

The number of spatial associations between the ROMA-BZCAT and the VLSS sources is 697 out of the 2727 (i.e.,  $\sim 26\%$ ), all unique matches within  $R_A$ . The probability of spurious associations, evaluated by shifting the coordinates of the ROMA-BZCAT blazars in random direction of the sky by  $1'$ , is extremely small being less

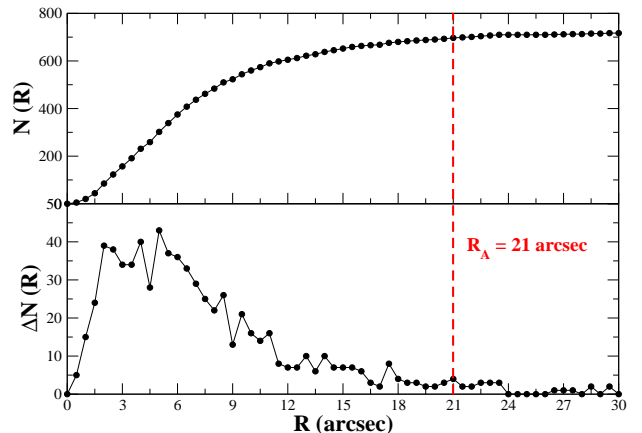


FIG. 1.— Upper panel) The number of total matches  $N(R)$  as a function of the radius  $R$  between  $0''$  and  $30''$ . Lower panel) The difference  $\Delta N(R)$  between the number of associations at given radius  $R$  and those at  $R - \Delta R$  as a function of the radius  $R$  in the same range of the above plot. The radial threshold  $R_A$  selected for our ROMA-BZCAT - VLSS crossmatches is indicated by the vertical dashed red line (see Section 2 for more details).

TABLE 1  
BLAZAR SAMPLES.

Sample	BZBs	BZQs	BZUs	Total
Blazars at Dec. $> -30^\circ$	1115	1412	200	2727
VLB sample	128	495	74	697
Fermi blazars at Dec. $> -30^\circ$	349	282	47	678
VLGB sample	67	145	21	233

than 0.1% (see Maselli et al. 2010, and references therein for details on the method to estimate the fraction of spurious associations).

## 3. SAMPLE SELECTION

We have defined two samples of blazars to carry out our analysis as described below. The main sample, labeled as VLSS Blazar (VLB) sample, contains 697 blazars with a unique radio counterpart in the VLSS within  $21''$ , while the subsample, labeled as VLSS Gamma-ray Blazar (VLGB) lists only the 233  $\gamma$ -ray emitting blazars out of 697 sources.

In Figure 2 we show the scatter plot of the angular separation between the ROMA-BZCAT positions and that of the VLSS catalog as a function of the integrated flux density,  $S_{74}$ , for the whole VLB sample. As expected, there is a mild trend between these two quantities because the position of faint VLSS sources are less accurately determined (e.g., Cohen et al. 2007). In addition, a larger population of weak sources against which the cross-identification could fail to identify the correct counterpart might be also present. All the blazar samples previously described are summarized in Table 1.

## 4. BLAZAR SPECTRAL PROPERTIES AT 74 MHz

### 4.1. Spectral shape at 74 MHz

The ROMA-BZCAT blazars are associated with NVSS or FIRST counterparts so their flux density at 1.4 GHz:

<sup>7</sup> [www.asdc.asi.it/bzcat/](http://www.asdc.asi.it/bzcat/)

<sup>8</sup> <http://heasarc.gsfc.nasa.gov/W3Browse/all/vlss.html>

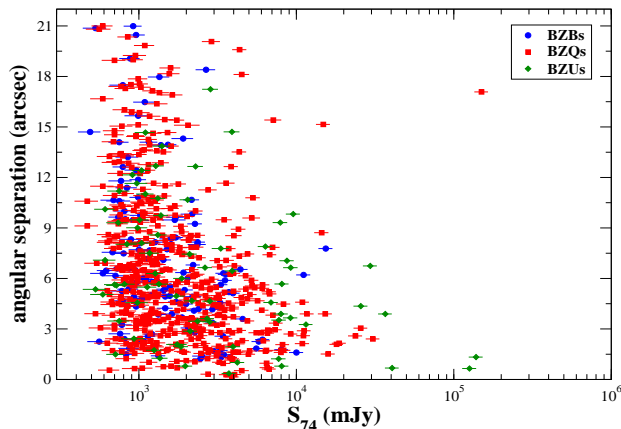


FIG. 2.— The angular separation between the ROMA-BZCAT positions and that of the VLSS catalog versus the flux density at 74 MHz,  $S_{74}$ , for the whole VLB sample.

$S_{1400}$  is available in the catalog. In particular, for 692 out of the 697 in the VLB sample the flux at 4.85 GHz is also reported in the ROMA-BZCAT. Thus we calculated the following two radio spectral indices:  $\alpha_{74}^{1400}$  between 74 MHz and 1.4 GHz and that  $\alpha_{1400}^{4850}$  between 1.4 GHz and 4.85 GHz and we also computed the difference:

$$\Delta\alpha = \alpha_{1400}^{4850} - \alpha_{74}^{1400} . \quad (2)$$

Thus, sources with  $\Delta\alpha < 0$  show radio spectral shapes that steepen moving toward low frequencies while those with  $\Delta\alpha > 0$  appear to be flatter below 1.4 GHz than they are at high radio frequencies. The relative uncertainties on the radio flux densities are  $\sim 13\%$ ,  $3\%$  and  $9\%$  at 74 MHz, 1.4 GHz and 4.85 GHz respectively, in particular being systematically lower than 10. This corresponds to a mean uncertainty on the spectral indices of 0.04 and 0.08 for  $\alpha_{74}^{1400}$  and  $\alpha_{1400}^{4850}$ , respectively and to a mean error on  $\Delta\alpha$  of 0.09<sup>9</sup>. Thus the uncertainties on the spectral indices are definitively not affecting our analysis since the standard deviation of the distributions for the entire VLB sample is systematically larger than them.

In Figure 3, we show the distribution of the  $\alpha_{74}^{1400}$  for the blazars in the VLB sample distinguishing between the BZBs and BZQs. The large fraction of radio spectral indices,  $\alpha_{74}^{1400}$ , for blazars are systematically smaller than 1.0 (i.e.,  $\sim 99\%$ ), with the 80% lower than  $\sim 0.75$ . In particular, the two  $\alpha_{74}^{1400}$  distributions for the BZBs and the BZQs appear to be similar at 99% level of confidence according to a Kolmogorov-Smirnov (KS) test. These distributions indicate that they have relatively flat radio spectra also at frequencies below 100 MHz, in agreement with their behavior at 325 MHz (Massaro et al. 2013). The flatness of the blazar radio spectra is expected from the high radio frequency data in the GHz energy range (e.g., Healey et al. 2007; Ivezić et al. 2002; Kimball & Ivezić 2008) and this spectral property was also used for the identification of  $\gamma$ -ray

<sup>9</sup> For  $\alpha = \log(S_2/S_1)/\log(\nu_2/\nu_1)$  the correspondent error is  $\sigma_\alpha = 1/\log(\nu_2/\nu_1)/\ln(10) \cdot \sqrt{\rho_1^2 + \rho_2^2}$  where  $\rho_i = \sigma_i/S_i$  (with  $i=1,2$ ) is the relative error on each flux density.

### VLB sample

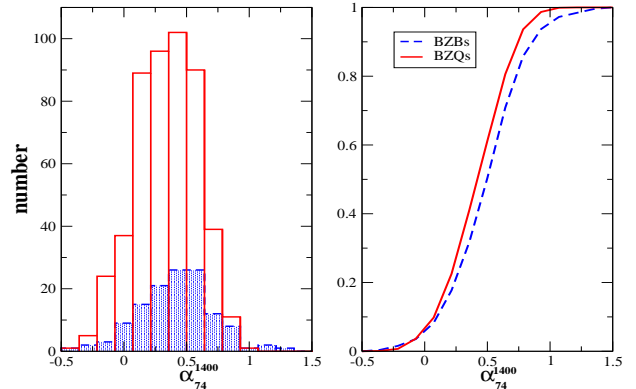


FIG. 3.— Left panel) The distributions of the radio spectral index  $\alpha_{74}^{1400}$  for blazars in the VLB sample, BZBs (blue) and BZQs (red). Right panel) The cumulative distribution for the same sample.

### VLGB sample

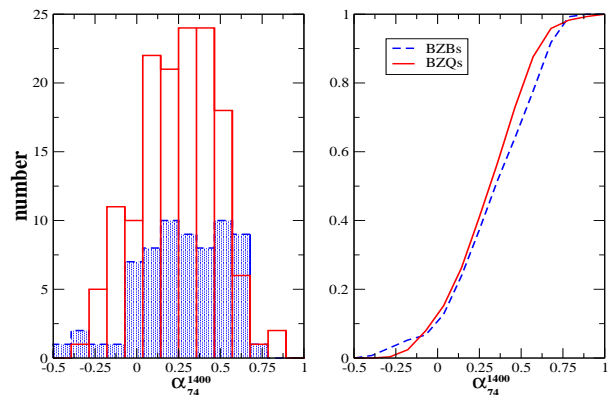


FIG. 4.— Left panel) The distribution of the radio spectral index  $\alpha_{74}^{1400}$  of all the blazars in the VLGB sample, BZBs (blue) and BZQs (red). Right panel) The cumulative distribution for the same sample.

sources since the EGRET era (e.g., Mattox et al. 1997). However, low-frequency radio observations, as those of the VLSS at 74 MHz were never previously investigated to confirm this trend for a systematic study of the blazar population.

In Figure 4, we show the comparison between the BZB and the BZQ spectral index distributions considering only  $\gamma$ -ray blazars in the VLGB sample. Here we note that all the *Fermi* detected blazars have spectral indices systematically flatter than those in the VLB sample. As observed in the VLB sample (see Figure 3), a KS test indicates that also in this case these two  $\alpha_{74}^{1400}$  distributions of BZBs and BZQs in the VLGB sample are similar at 99% level of confidence. In addition, we did not find any correlation or net trend between the  $\alpha_{74}^{1400}$  and the  $\gamma$ -ray spectral index  $\alpha_\gamma$  for the whole VLGB sample.

### 4.2. Flux densities at 74 MHz

We computed the distributions of the  $S_{74}$  flux densities comparing the BZBs and the BZQs for the VLB sample

## VLB sample

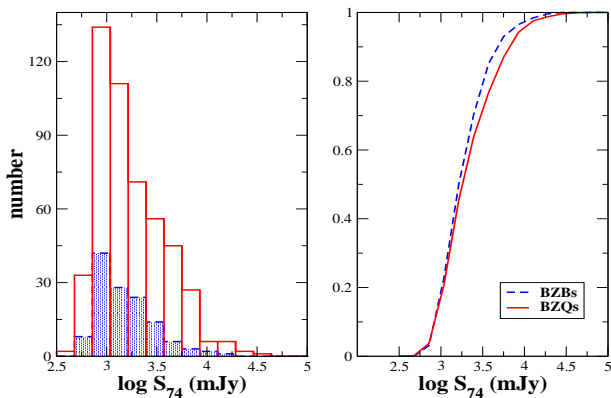


FIG. 5.— Left panel) The distributions of the low-frequency radio flux density  $S_{74}$  for the blazars in the VLB sample. The BZB and BZQ distributions appear statistically similar according to the KS test. Right panel) The cumulative distribution for the same sample.

as shown in Figure 5, that appear similar at 99% level of confidence evaluated according to a KS test. In Figure 6 we show the scatter plot of the NVSS flux density at 1.4 GHz  $S_{1400}$  with respect to that at 74 MHz  $S_{74}$  where it is worth noting that 99% of the blazars detected in the VLB sample have  $S_{1400}=0.05\times S_{74}$ , as indicated by the black dashed line.

For the blazars in the VLGB sample, we also searched for a trend between the radio and the  $\gamma$ -ray emissions (e.g., Ghirlanda et al. 2010; Mahony et al. 2010; Ackermann et al. 2011b) as we did previously using the WENSS observations at 325 MHz (Massaro et al. 2013); however, as shown in Figure 7 there is not a clear trend or correlation between the  $\gamma$ -ray and the radio flux density at 74 MHz.

We remark that only 697 out of 2727 ROMA-BZCAT sources have a unique association in the VLSS survey within a radius of  $21''$ , thus  $\sim 74\%$  of them were not associated or either not detected at 74 MHz. Most of

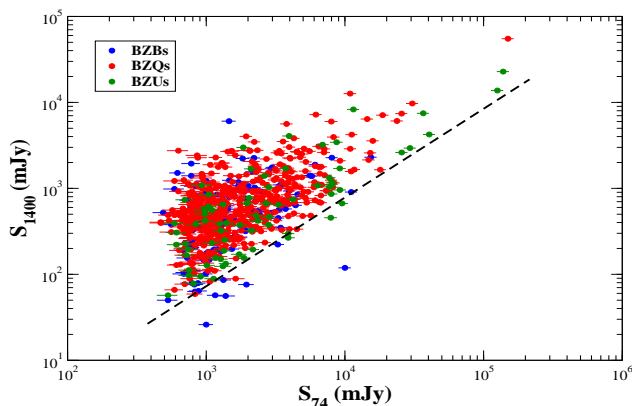


FIG. 6.— The scatter plot between the  $S_{1400}$  and  $S_{74}$  radio flux densities. The BZBs (blue circles), BZQs (red square) and BZUs (green diamonds) are shown separately. The black dashed line corresponds to the power-law:  $S_{1400}=0.05\times S_{74}$ .

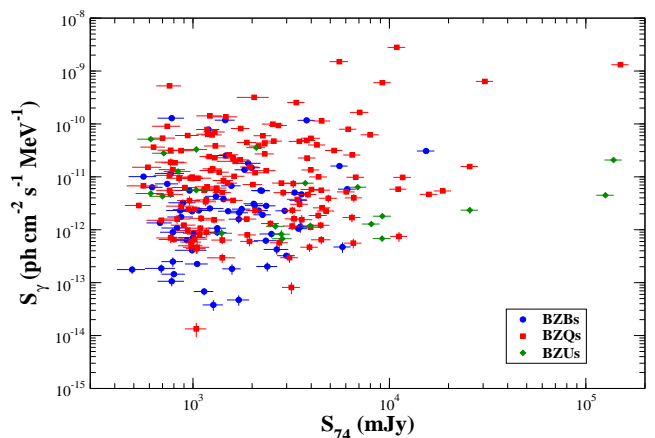


FIG. 7.— The scatter plot of the  $\gamma$ -ray flux density *vs* radio 74 MHz for the BZBs (blue), the BZQs (red) and the BZUs (green) that belong to the VLGB sample (see Section 4.2 for more details).

these undetected blazars could lie below the completeness threshold of the VLSS, that for the 50% point-source detection limit is roughly 0.7 Jy for a typical noise level of 0.1 Jy/beam, evaluated taking into account both ionospheric smearing and the clean bias (Cohen et al. 2007). In addition, the noise levels are not constant throughout the survey region and only the differential completeness as a function of signal-to-noise ratio has been defined (see Section 8 of Cohen et al. 2007, for more details). Consequently, it is not possible to extrapolate the  $S_{1400}$  flux densities to 74 MHz to test if blazars with no VLSS counterparts lie above or below the completeness of the survey. This situation is even more complicated because blazars could be variable at 74 MHz making any expectation less reliable.

However, to evaluate if we should expect to detect the remaining 2030 blazars, we assigned a spectral index  $\alpha_{74}^{1400}$  equal to the peak of the spectra index distributions of the BZBs, BZQs and BZUs in the VLB sample to those blazars that do not have a VLSS counterpart within  $21''$  and we computed the extrapolated  $S_{74}^*$  flux density on the basis of their measured  $S_{1400}$ . We adopted a value of  $\alpha_{74}^{1400}$  equal to 0.43, 0.34 and 0.51 for the BZBs, the BZQs and the BZUs, respectively. Comparing the VLSS radio sources with the blazars in the VLB sample we found that 63% of the VLSS objects have flux densities  $S_{74}$  greater than  $\sim 1$ Jy while only  $\sim 16\%$  of the undetected blazars have extrapolated  $S_{74}^*$  above this threshold, indicating that the large fraction of them are not expected to have a counterpart in the VLSS as occurs.

## 5. DISCUSSION AND CONCLUSIONS

We investigated the distribution of the radio spectral index  $\alpha_{74}^{1400}$  for the blazars with a VLSS counterpart also focusing on those that are associated with  $\gamma$ -ray sources. We found that about 60% of  $\gamma$ -ray emitting blazars have flat radio spectra (i.e.,  $\alpha_{74}^{1400} < 0.5$ ), with 99% even smaller than 0.9 (see Section 4.1 for more details) as occurs when analyzing radio data at higher frequency (e.g., Healey et al. 2007; Massaro et al. 2013). This strongly suggests that blazar spectra are still dominated by the beamed radiation arising from particles accelerated in

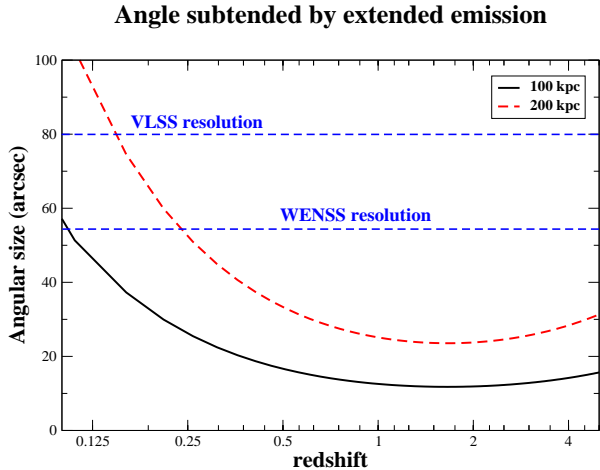


FIG. 8.— The angle subtended by extended structures of 100 kpc (black line) and 200 kpc (red dashed line), respectively as a function of the redshift. The two horizontal blue dashed lines represent the typical angular resolution of the WENSS (Rengelink et al. 1997) and VLSS (Cohen et al. 2007) surveys. It is clear that for blazars at redshifts larger than  $\sim 0.1$ , extended structures of size smaller than 200 kpc cannot be resolved. This indicates that the flux densities measured at low radio frequencies arise from both nuclear and large scale components. The 100 kpc and 200 kpc size are representative of the scale observed in radio galaxies.

their relativistic jets even at 74 MHz, in agreement with the recent results of Kimball et al. (2011).

There are several implications of our results in the context of the unification scenario of radio-loud AGNs. In 1974 Fanaroff and Riley proposed the classification scheme for the extragalactic radio sources distinguishing two classes on the basis of the correlation between the relative positions of regions of high and low surface brightness in their extended components (Fanaroff & Riley 1974). They introduced the ratio  $R_{FR}$  of the distance between the regions of highest surface brightness on opposite sides of the central galaxy and/or quasar, to the total extent of the source up to the lowest brightness contour in the radio map. Sources with  $R_{FR} \leq 0.5$  were placed in Class I (i.e., FRI) and sources with  $R_{FR} \geq 0.5$  in Class II (i.e., FR II). At radio frequencies, FRIs show surface brightness higher toward their cores while FR IIs toward their edges. It was also found that nearly all sources with luminosity  $L_{178MHz} \leq 2 \times 10^{25} h_{100}^{-2} \text{ W Hz}^{-1} \text{ str}^{-1}$  were FRI while the brighter sources were nearly all of FR II. The luminosity boundary between them is not very sharp, and there is some overlap in the luminosities of sources classified as FRI or FR II on the basis of their structures.

Several observational evidences support the idea originally proposed by Blandford & Königl in 1979 that suggested powerful FR II radio galaxies as the parent populations of BZQs while BZBs were assumed intrinsically similar to weak FR Is (e.g., Urry & Padovani 1995; Scarpa & Urry 2001, and reference therein for more details). Both radio galaxies and blazars have similar host galaxies: giant ellipticals (e.g., Scarpa & Urry 2000a; Scarpa & Urry 2000b) and deep radio observations of selected blazars at 1.4 GHz show extended structures remarkably similar to those of lobes and plumes of radio galaxies (e.g.

Antonucci & Ulvestad 1995). Thus, according to the unification scenario of radio-loud active galaxies (e.g., Blandford & Rees 1978b; Blandford & Königl 1979; Urry & Padovani 1995), radio galaxies are generally interpreted as misaligned blazars.

The low-frequency radio observations of blazars presented here allow us to make a direct test of the unification scenario of radio-loud active galaxies and of the blazars – radio galaxies connection. At MHz frequencies radio galaxies clearly show steep radio spectra as for example highlighted in the Third Cambridge Catalog of radio sources (3C; Edge et al. 1959; Spinrad et al. 1985) by Kellerman et al. (1968) and Pauliny-Toth et al. (1968) (see also Kellerman et al. 1969; Kellerman & Pauliny-Toth 1969). The main reason underlying this spectral behavior is due to the combination of emission arising from compact cores, having typically flat radio spectra, with that of extended structures, such as plumes (in FR Is) or lobes (in FR IIs) characterized by steep radio spectra. Consequently, their combined spectra at low-frequency, such as at 74 MHz, where the large beam of the radio surveys does not allow us to resolve different components, is dominated by that of large (i.e., kpc) scale structures thus resulting in steep radio spectra. In particular, Figure 8 shows the angle subtended by 100 kpc and 200 kpc extended structures as a function of redshift  $z$ . It is clear that above  $z \sim 0.1$ , both the VLSS and the WENSS surveys cannot distinguish the emission arising from the core and from the extended components in radio galaxies and blazars. Thus flux densities measured at 74 MHz include both these contributions.

Since the emission arising from large scale structures is isotropic, it is not dependent on the orientation relative to the line of sight. So, according to the unification scenario, we expect to detect steep radio spectra, typical of extended components, also when observing blazars at low radio frequencies as occurs in radio galaxies. To describe the above situation we can consider the schematic representation of the radio spectra of a BZQ in comparison with that of an FR II radio galaxy as shown in Figure 9. Given the resolution of the low frequency radio surveys (e.g., Figure 8) that cannot resolve and separate the contributions of extended and nuclear components, the integrated spectrum of a BZQ is expected to be similar to that of an FR II radio galaxy at low frequencies, unless the core emission is overcoming that of the extended structures (i.e.,  $\Delta\alpha > 0$ ).

In order to test these expectations of the unification scenario we computed the  $\Delta\alpha$  for all the sources in the VLB sample that have data at 4.85 GHz as reported in the ROMA-BZCAT. In Figure 10, we show the distribution of the  $\Delta\alpha$  for the BZBs and the BZQs; it is quite evident that the large fraction of the VLB sources (i.e.,  $\sim 70\%$ ) show the spectral shape expected by the interpretation of blazars being intrinsically similar to radio galaxies. In addition, we plot the  $\Delta\alpha$  as a function of the radio spectral index evaluated at high frequencies  $\alpha_{1400}^{4850}$  (Figure 11) and of the radio flux density at 1.4 GHz  $S_{1400}$  (Figure 12). These two additional plots also show trends in agreement with the unification scenario of radio-loud sources, since radio emission from steep components tend to be more evident in blazars with flatter or even inverted radio spectra (see also Figure 11) and brighter sources

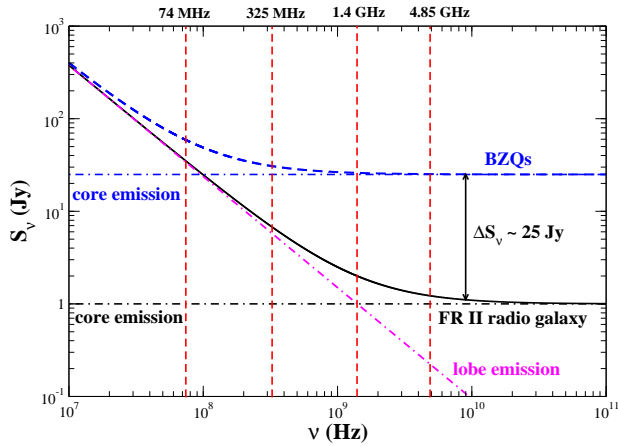


FIG. 9.— *Left panel*) The schematic view of the integrated radio spectrum of an FR II radio galaxy (black curve) in comparison with that of a BZQ (blue curve), assuming the same emission arising from their extended structures. The flat spectrum core emission showing dominates at high frequencies while the steep spectrum of the extended structures (i.e., lobes) overcomes the nuclear radio at low frequencies. However, since BZQs show relatively flat spectra at low radio frequencies the core emission has to be much brighter than that of the FR II radio galaxy, as for example, up to a factor of  $\sim 25$  when compared at  $\sim 5$  GHz. This scenario is in agreement with the expectations of the unification scenario of radio-loud active galaxies.

tend to maintain their flat spectra also at low frequencies, according to the fact that their nuclear beamed radiation overwhelms that arising from their extended structures. However, one controversy arises from the above results. It is indeed clear the presence of blazars with counterparts for which the  $\Delta\alpha > 0$ . This spectral difference could be interpreted as, for example, due to synchrotron self absorbed components in the blazar compact cores, or to intrinsic source variability of the epochs when the

### VLB sample

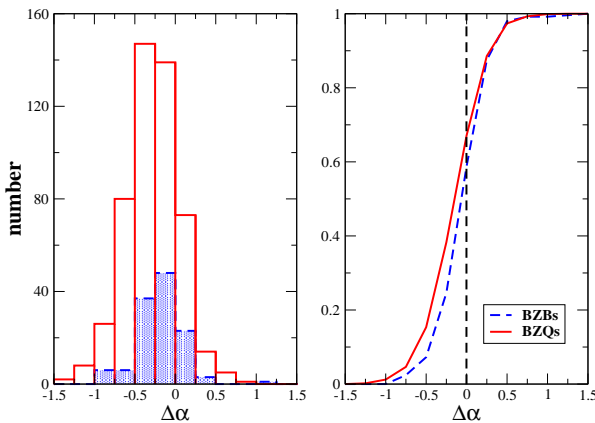


FIG. 10.— The distribution of the  $\Delta\alpha = \alpha_{4850}^{1400} - \alpha_{74}^{1400}$  for the BZBs (blue) and the BZQs (red) in the VLB sample for which radio data at 4.85 GHz are available (i.e., 692 out of 697 sources). The cumulative distribution is also shown on the right panel. The dashed vertical black line corresponds to the dividing sign between blazars that become steeper ( $\Delta\alpha < 0$ ) or flatter ( $\Delta\alpha > 0$ ) at low frequencies that they are above 1.4 GHz.

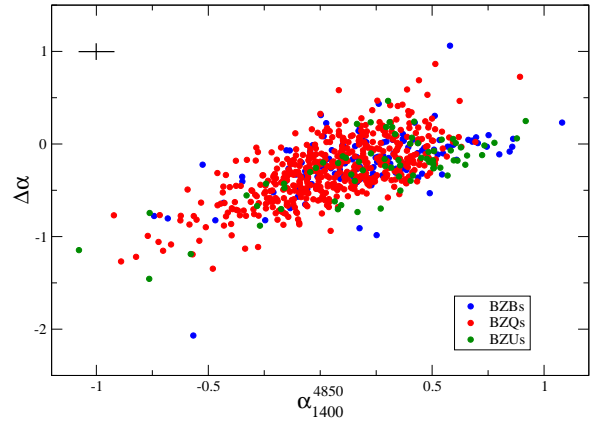


FIG. 11.— The scatter plot of the spectral index variation  $\Delta\alpha$  as a function of  $\alpha_{4850}^{1400}$  for BZBs (blue circles), BZQs (red squares) and BZUs (green diamond), respectively. Blazars with flatter radio spectra tend to have steep components dominating at low frequencies below 1.4 GHz. The black cross indicates the typical uncertainty on the  $\Delta\alpha$  and  $\alpha_{4850}^{1400}$  values.

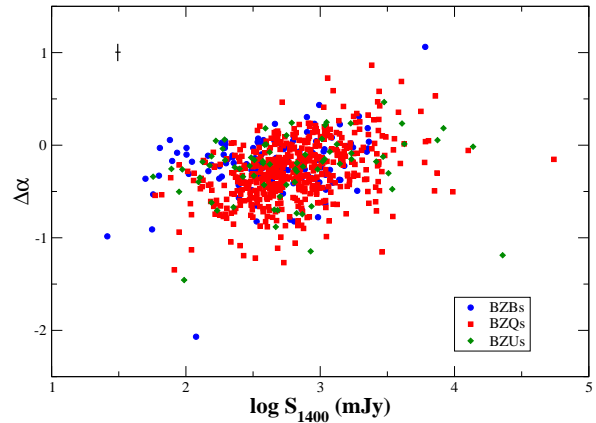


FIG. 12.— The scatter plot of the spectral index variation  $\Delta\alpha$  as a function of the radio flux density at 1.4 GHz  $S_{1400}$  for BZBs (blue circles), BZQs (red squares) and BZUs (green diamond), respectively. Blazars bright at 1.4 GHz tend to hide the emission arising from extended structures (i.e., steep components) at low frequencies below 1.4 GHz. The black cross indicates the typical uncertainty on the  $\Delta\alpha$  and  $S_{1400}$  values.

radio observations were taken, since they are not simultaneous.

In particular, blazars show intrinsic variability over a wide range of wavelengths and their flux variations, even at radio wavelengths, occur stochastically, so this could affect the estimate of the spectral indices. However, the VLB sample is selected on the basis of the source detection at 74 MHz implying that these blazars have 1.4 GHz and 4.85 GHz flux densities well above the sensitivity limit of the high-frequency radio surveys. We expect that the flux densities measured at 1.4 GHz and 4.85 GHz are well representative and thus the spectral indices between these two frequencies are also well rep-

representative of the average state of the source. In the X-ray band, this generic survey property has been extensively used to select blazars as targets for investigating the absorption lines in the warm hot intergalactic region (see e.g., Nicastro et al. 2003; Nicastro et al. 2005; Nicastro et al. 2013).

Consequently, given the absence of any duty cycle in the blazar variability pattern and the random occurrence of their flaring activity, for each VLB source having a  $\Delta\alpha > 0$ , due, for example, to a high state occurring while measuring the flux density at 1.4 GHz, we could expect a blazar with  $\Delta\alpha < 0$  due to a flare at 74MHz while the VLSS observations were performed.

In addition, the scatter induced on the  $\Delta\alpha$  distribution remains below  $\sim 0.17$ , i.e., half as small as the standard deviation of the real distribution ( $\sim 0.33$ , see Figure 10), for flux variations up to a factor of 1.5. This value is larger than the typical variations observed for most blazars over the course of a dedicated multi-year monitoring at 15 GHz, where the flux changes are expected to be even larger than those at 1.4 GHz or below (Richards et al. 2011).

Thus the presence of VLB sources with  $\Delta\alpha > 0$ , if not affected by variability, is not completely in agreement with the unification scenario of radio-loud active galaxies since it would imply the presence of an appreciable fraction of blazars for which radio emission from extended structures (plumes and/or lobes) is not detected (as indeed expected).

This discovery could imply new insights on the unification scenario of radio-loud active galaxies opening new questions as for example: i) is the distinction between blazars and radio galaxies driven not only by the orientation along the line of sights but also by a different parameter or a combination of them? (e.g., accretion rate, black hole mass) ii) Is it possible that the difference between radio-loud active galaxies could be also due to their surrounding environments? The unsolved issues deserve further investigation to confirm the peculiar spectral behavior of blazars. Independent analysis can be carried out using the low frequency observations of the Murchison Widefield Array (MWA) (Tinagy et al. 2013) radio telescope combined with existing Australia Telescope Compact Array (ATCA) surveys at 20 GHz (e.g., Frater et al. 1992; Murphy et al. 2010; Massardi et al. 2011). Future investigations with the new generation of low-frequency radio telescopes as the LOW Frequency ARray (LOFAR) (e.g., van Haarlem et al 2013), the Square Kilometer Array (SKA) (e.g., Dewdney et al. 2010) will also be crucial to resolve nuclear and extended components in blazars.

We thank our anonymous referee for many helpful comments and for stimulating the discussion on the possible effects of the variability, which greatly improved this manuscript. We thank R. Morganti and D. Harris for their valuable comments and suggestions. F. Massaro is grateful to S. Digel, E. Mahony, M. Murgia, Howard Smith and M. Urry for their helpful discussions. The work is supported by the NASA grants NNX12AO97G. R. D’Abrusco gratefully acknowledges the financial support of the US Virtual Astronomical Observatory, which is sponsored by the National Science Foundation and the National Aeronautics and Space Administration. The work by G. Tosti is supported by the ASI/INAF contract I/005/12/0. The WENSS project was a collaboration between the Netherlands Foundation for Research in Astronomy and the Leiden Observatory. We acknowledge the WENSS team consisted of Ger de Bruyn, Yuan Tang, Roeland Rengelink, George Miley, Huub Rottgering, Malcolm Bremer, Martin Bremer, Wim Brouw, Ernst Raimond and David Fullagar for the extensive work aimed at producing the WENSS catalog. Part of this work is based on archival data, software or on-line services provided by the ASI Science Data Center. This research has made use of data obtained from the High Energy Astrophysics Science Archive Research Center (HEASARC) provided by NASA’s Goddard Space Flight Center; the SIMBAD database operated at CDS, Strasbourg, France; the NASA/IPAC Extragalactic Database (NED) operated by the Jet Propulsion Laboratory, California Institute of Technology, under contract with the National Aeronautics and Space Administration. Part of this work is based on the NVSS (NRAO VLA Sky Survey) and on the VLA low-frequency Sky Survey (VLSS); The National Radio Astronomy Observatory is operated by Associated Universities, Inc., under contract with the National Science Foundation. This publication makes use of data products from the Two Micron All Sky Survey, which is a joint project of the University of Massachusetts and the Infrared Processing and Analysis Center/California Institute of Technology, funded by the National Aeronautics and Space Administration and the National Science Foundation. This publication makes use of data products from the Wide-field Infrared Survey Explorer, which is a joint project of the University of California, Los Angeles, and the Jet Propulsion Laboratory/California Institute of Technology, funded by the National Aeronautics and Space Administration. TOPCAT<sup>10</sup> (Taylor 2005) for the preparation and manipulation of the tabular data and the images.

Facilities: VLA, WSRT

## REFERENCES

- Ackermann, M. et al. 2011a ApJ, 743, 171  
 Ackermann, M. et al. 2011b ApJ, 741, 30  
 Antonucci, R. R. J., Ulvestad, J. S. 1985 ApJ, 294, 158  
 Artyukh, V. S. & Vetukhnovskaya, Y. N. 1981 SvA, 25, 397  
 Becker, R. H., White, R. L., Helfand, D. J. 1995 ApJ, 450, 559  
 Blandford, R. D., Rees, M. J., 1978a, PROC. Pittsburgh Conference on BL Lac objects”, 328  
 Blandford, R. D., Rees, M. J., 1978b PhysS, 17, 265  
 Blandford, R. D. & Königl, A. 1979 ApJ, 232, 34  
 Cohen, A. S., Lane, W. M., Cotton, W. D., Kassim, N. E., Lazio, T. J. W., Perley, R. A., Condon, J. J., Erickson, W. C. 2007 AJ, 134, 1245  
 Condon, J. J., Cotton, W. D., Greisen, E. W., Yin, Q. F., Perley, R. A., Taylor, G. B., & Broderick, J. J. 1998, AJ, 115, 1693  
 D’Abrusco, R., Massaro, F., Ajello, M., Grindlay, J. E., Smith, Howard A. & Tosti, G. 2012 ApJ, 748, 68  
 D’Abrusco, R., Massaro, F., Paggi, A., Masetti, N., Giroletti, M., Tosti, G., Smith, Howard, A. 2013 ApJS submitted  
 Dewdney, P., et al. 2010, SKA Memo # 130, SKA Phase 1: Preliminary System Description  
 Dunkley, J., et al. 2009 ApJS, 180, 306

<sup>10</sup> <http://www.star.bris.ac.uk/~mbt/topcat/>

- Edge, D. O., Shakeshaft, J. R., McAdam, W. B., Baldwin, J. E.; Archer, S. 1959 MmRAS, 68, 37
- Fanaroff, B. L. & Riley J. M. 1974, MNRAS, 167, P31
- Frater R. H., Brooks J. W., 1992, J. Electr. Electron. Eng., 12, 100
- Ghirlanda, G., Ghisellini, G., Tavecchio, F., Foschini, L. 2010 MNRAS, 407, 791
- Healey, S. E. et al. 2007 ApJS, 171, 61
- Ivezic, Z. et al. 2002 AJ, 124, 2364
- Kellermann, K. I., Pauliny-Toth, I. I. K., Tyler, W. C. 1968 AJ, 73, 298
- Kellermann, K. I., Pauliny-Toth, I. I. K., Williams, P. J. S. 1969 ApJ, 157, 1
- Kellermann, K. I. & Pauliny-Toth, I. I. K. 1969b ApJ, 155L, 71
- Kharb, P., Lister, M. L., Cooper, N. J. 2010 ApJ, 710, 764
- Kimball, A. & Izevic, Z. 2008 AJ, 136, 684
- Laurent-Muehleisen, S. A., Kollgaard, R. I., Feigelson, E. D., Brinkmann, W., Siebert, J. 1999 ApJ, 525, 127
- Mahony, E. K., Sadler, E. M., Murphy, T., Ekers, R. D., Edwards, P. G., Massardi, M. 2010 ApJ, 718, 587
- Maselli, A., Massaro, E., Nesci, R., Sclavi, S., Rossi, C., Giommi, P. 2010 A&A, 512A, 74
- Massardi, M. et al., 2011, MNRAS, 412, 318.
- Massaro, F., D'Abrusco, R., Ajello, M., Grindlay, J. E. & Smith, H. A. 2011a ApJ, 740L, 48
- Massaro, E., Giommi, P., Leto, C., Marchegiani, P., Maselli, A., Perri, M., Piranomonte, S., Sclavi, S. 2009 A&A, 495, 691
- Massaro, E., Giommi, P., Leto, C., Marchegiani, P., Maselli, A., Perri, M., Piranomonte, S., 2011b "Multifrequency Catalogue of Blazars (3rd Edition)", ARACNE Editrice, Rome, Italy
- Massaro, F., D'Abrusco, R., Giroletti, M., Paggi, A., Masetti, N., Tosti, G., Smith, Howard, A. 2013a ApJS accepted
- Mattox, J. R. et al. 1997 Apj, 481,95
- Murphy, T. et al. 2010, MNRAS, 402, 2403
- Nicastro, F., Zezas, A., Elvis, M., et al. 2003 Nature, 421, 719
- Nicastro, F., Mathur, S., Elvis, M., et al., 2005 ApJ, 629, 700
- Nicastro, F. et al. 2013 ApJ, 769, 90
- Nolan et al. 2012 ApJS, 199, 31
- Pauliny-Toth, I. I. K. & Kellermann, K. I. 1968 AJ, 73, 953
- Rengelink, R. et al. 1997, A&A Suppl. 124, 259
- Richards, J. L. et al. 2011, 194, 29
- Scarpa, R.; Urry, C. M., Falomo, R., Pesce, Joseph E., Treves, A. 2000a ApJ, 532, 740
- Scarpa, R.; Urry, C. M.; Padovani, P.; Calzetti, D.; O'Dowd, M. 2000b ApJ, 544, 258
- Scarpa, R. & Urry, C. M. 2001 ApJ, 556, 749
- Spinrad, H., Marr, J., Aguilar, L., Djorgovski, S. 1985 PASP, 97, 932
- Stickel, M., Padovani, P., Urry, C. M., Fried, J. W., Kuehr, H. 1991 ApJ, 374, 431
- Stocke et al. 1991, ApJS, 76, 813
- Taylor, M. B. 2005, ASP Conf. Ser., 347, 29
- Tingay S. J. et al. 2013 PASA, 30, 7
- Urry, C. M., & Padovani, P. 1995, PASP, 107, 803
- van Haarlem, M. P. et al. 2013 A&A accepted for publication (arXiv:1305.3550)
- White, R. L., Becker, R. H. Helfand, D. J., Gregg, M. D. et al. 1997 ApJ, 475, 479